Acta Cryst. (1956). 9, 131

X-ray and Neutron Diffraction Study of Ferroelectric $PbTiO_3$

BY GEN SHIRANE AND RAY PEPINSKY

Department of Physics, The Pennsylvania State University, University Park, Pennsylvania, U.S.A.

AND B. C. FRAZER

Department of Physics, Brookhaven National Laboratory, Upton, Long Island, N.Y., U.S.A.

(*Received* 18 *May* 1955 *and in revised form* 20 *June* 1955)

X-ray single-crystal and neutron powder diffraction analyses of tetragonal $PbTiO_3$ at room temperature reveal the following coordinate shifts of the Ti and O atoms from perovskite positions, with Pb taken at the origin of the pseudo-perovskite cell:

$$\delta z_{Ti} = +0{\cdot}040,\ \delta z_{O_I} = +0{\cdot}112,\ \delta z_{O_{II}} = +0{\cdot}112\ .$$

The equivalence of δz_{O_I} and $\delta z_{O_{II}}$ suggests that the oxygen octahedra may be considered as 'fixed' in the lattice as the crystal passes from the cubic paraelectric phase above 490° C. to the tetragonal ferroelectric structure which it maintains below this temperature. With the oxygens defining the cell, the Pb ions are shifted by +0·47 Å along the z axis, and the Ti ions move in the same direction by 0·30 Å.

This structure is compared to previous results of X-ray and recent neutron single-crystal studies of tetragonal $BaTiO_3$.

1. Introduction

In recent years a considerable amount of experimental and theoretical study has been directed at ferroelectric $BaTiO_3$ (see, for example, Devonshire, 1954). The very simple structure-type of this crystal, as compared with other ferroelectrics such as Rochelle salt and KH_2PO_4, gave hope of a better understanding of the nature of ferroelectric properties. Solution of the structure of the ferroelectric phases of this crystal turned out to be a very difficult matter, however. $BaTiO_3$ has a cubic perovskite-type structure above the Curie temperature, 120° C. (see Fig. 1). It is distorted, at room

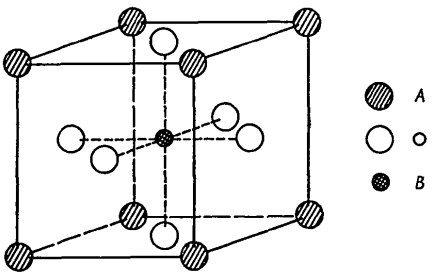

Fig. 1. Cubic perovskite-type structure.

temperature, to a tetragonal lattice (Megaw, 1946) with:

$$a = 3{\cdot}986,\ c = 4{\cdot}026\ \text{Å};\ c/a = 1{\cdot}01;$$
$$\text{space group } C_{4v}^1\text{–}P4mm\ .$$

Taking Ba at the origin, the atomic positions can be described in terms of the three parameters δz_{Ti}, δz_{O_I} and $\delta z_{O_{II}}$. The coordinates for all the atoms are then:

Ba at (0, 0, 0),
Ti at $(\frac{1}{2}, \frac{1}{2}, \frac{1}{2}+\delta z_{Ti})$,
O_I at $(\frac{1}{2}, \frac{1}{2}, \delta z_{O_I})$,
O_{II} at $(\frac{1}{2}, 0, \frac{1}{2}+\delta z_{O_{II}})$ and $(0, \frac{1}{2}, \frac{1}{2}+\delta z_{O_{II}})$.

These three atomic coordinate parameters, together with nine anisotropic temperature parameters, give the whole picture of the structure.

The first X-ray study, by Kaenzig (1951), assumed $\delta z_{O_{II}} = 0$, and gave $\delta z_{Ti} = +0{\cdot}014$, $\delta z_{O_I} = -0{\cdot}032$. A subsequent detailed analysis by Evans (1953) led that investigator to conclude that, within a rather wide range, it was not possible to determine the structure uniquely by X-rays, because of the interaction between coordinate and thermal oscillation parameters along the z axis. After some assumptions concerning temperature parameters, Evans gave the most reasonable parameters as $\delta z_{Ti} = +0{\cdot}012$, $\delta z_{O_I} = -0{\cdot}026$ and $\delta z_{O_{II}} = 0$. But it was shown that a model with $\delta z_{Ti} = +0{\cdot}015$, $\delta z_{O_I} = -0{\cdot}024$ and $\delta z_{O_{II}} = -0{\cdot}020$ also gave good agreement, though the temperature factors were quite unreasonable for this model. These two structures of Evans will be referred to hereafter as Evans' first and second structures respectively.

Kaenzig's structure, and Evans' first structure, gave a model in which Ba and two O_{II} are fixed, and Ti and O_I are shifted in a direction opposite to each other with O_I moving farther than Ti. This has been considered as the accepted model for the ferroelectric $BaTiO_3$, since theoretical considerations also favored it because of the character of the resulting Ti–O_I–Ti–O_I chain. In Evans' second model one could consider the oxygen octahedron network to be only slightly distorted, and thus to be more or less fixed in the tet-

ragonal lattice with respect to the non-ferroelectric cubic structure, and regard the Ti and Ba ions as shifting in the same direction, but with Ti moving farther than Ba.

Very recently, a neutron diffraction study of $BaTiO_3$ single crystals has been carried out by Frazer, Danner & Pepinsky (1955) at the Brookhaven reactor. Because of much more favorable relations between the values of the atomic scattering factors compared with the case of X-ray diffraction, a neutron diffraction study can provide more reliable atomic positions. Preliminary results reveal $\delta z_{\mathrm{Ti}} = +0{\cdot}014$, $\delta z_{\mathrm{O_I}} = -0{\cdot}023$ and $\delta z_{\mathrm{O_{II}}} = -0{\cdot}014$. Although these values may be subject to slight changes, they may be considered as the most reliable structure model for $BaTiO_3$ yet available. Compared with three models given by X-ray analysis, this model of Frazer *et al.* bears closest resemblance to Evans' second model.

Among the several other ferroelectrics of the $BaTiO_3$ type, $PbTiO_3$ is the only crystal which has a tetragonal modification at room temperature. The lattice constants are (Megaw, 1946; Náray-Szabó, 1943)

$$a = 3{\cdot}904,\ c = 4{\cdot}152\ \text{Å};\quad c/a = 1{\cdot}063\ .$$

The ferroelectric Curie temperature of this crystal is about 490° C. (Shirane & Hoshino, 1951; Rogers, 1953), at which point the structure changes from tetragonal to cubic in a manner similar to that in $BaTiO_3$. Moreover, a study of the mixed $BaTiO_3$–$PbTiO_3$ system (Shirane & Suzuki, 1951; Shirane & Takeda, 1951) revealed a continuous change of lattice constants and Curie temperature over the entire range of solid solutions. The anomaly of specific heat and a volume change at the Curie temperature also have the same characteristic for the entire range of solid solutions, with increasing anomaly towards the $PbTiO_3$ side. From this point of view, the ferroelectric properties of $BaTiO_3$ seem to be demonstrated in $PbTiO_3$ with magnification.

This enhancement of ferroelectric properties in $PbTiO_3$ must obviously result from the differences in properties of the Pb atom from those of Ba. Generally speaking, theoretical considerations have emphasized the role of Ti and O_I ions as the origin of ferroelectricity, and A ions (Ba or Pb) are considered to have less important contributions through their ionic size and polarizability. The ionic size is important in determining the packing of A ions with three oxygens, thus affecting the available space for Ti. This effect alone certainly cannot account entirely for the situation in $BaTiO_3$ and $PbTiO_3$, as is clearly demonstrated by the fact that $BaTiO_3$–$SrTiO_3$ shows a decrease of the Curie temperature with increasing Sr concentration; for the Sr ion is smaller than Ba, as is the Pb ion.

Because of its different electronic configurations and high atomic numbers, Pb is probably more polarizable and deformable than are the alkaline earth atoms Ba and Sr. It may also be true, as emphasized by Megaw (1954), that Pb cannot be treated as essentially ionic. As the first step in understanding the phenomenon, we have undertaken X-ray and neutron diffraction analyses of $PbTiO_3$, and have compared the result with the structure of $BaTiO_3$.

2. Analysis of the problem

It may be worth while to examine in detail the conditions which prevent the unique solution of the structure of $BaTiO_3$ by X-ray diffraction, and study the situation with $PbTiO_3$. For this purpose, the structure factor F of $PbTiO_3$ can be written as:

$$\begin{aligned} F &= A+iB \\ &= A(\mathrm{Pb})+A(\mathrm{Ti})+A(\mathrm{O})+i[B(\mathrm{Ti})+B(\mathrm{O})]\ , \\ \tan\alpha &= B/A\ , \end{aligned}$$

where, for example, $A(\mathrm{Pb})$ denotes the contribution of Pb atom to the real part A. The real part, A, contains only a linear combination of $\cos 2\pi l.\delta z$, and the imaginary part B contains $\sin 2\pi l.\delta z$ only. When all $\delta z = 0$, the structure factor has only real terms, as shown in Table 1.

Table 1. *Structure factors of (h0l) reflections for* $PbTiO_3$ *with all* δz*'s* $= 0$

$(h0l)$		F_{h0l}
$h = 2m$,	$l = 2n$	$f_{\mathrm{Pb}}+f_{\mathrm{Ti}}+3f_{\mathrm{O}}$
$h = 2m+1$,	$l = 2n+1$	$f_{\mathrm{Pb}}+f_{\mathrm{Ti}}-f_{\mathrm{O}}$
$h = 2m$,	$l = 2n+1$	$f_{\mathrm{Pb}}-f_{\mathrm{Ti}}-f_{\mathrm{O}}$
$h = 2m+1$,	$l = 2n$	

The two conditions which prevent the solution of $BaTiO_3$ structure are, according to Evans' discussion (1953): (1) all δz are so small that approximately $\cos 2\pi lz = 1$ and $\sin 2\pi lz = 2\pi lz$; (2) taking Ba at the origin, the phase angle α is small so that $\cos\alpha \cong 1$. This is due to the much larger scattering factor of Ba compared with those of Ti and O. When *both* of these conditions are satisfied, as in the case of the X-ray study of $BaTiO_3$, the interaction between the coordinate and the temperature parameters occurs and the structure cannot be solved without a rather wide range of uncertainty. In the case of neutron diffraction study, the second condition does not obtain, and the structure can be solved.

In the case of $PbTiO_3$, the first condition may not hold, since a larger δz is expected owing to the larger tetragonal distortion. The second condition of small α, however, certainly holds for an X-ray study, owing to the very dense Pb atom compared with Ti and O. Can the structure be solved uniquely in this case? The detailed study of the structure-factor formula has shown that the absolute value of the δz's can certainly be given, but it may be very difficult to determine their signs. This means, taking δz_{Ti} as positive (which we may always do), the combination of the sign of $\delta z_{\mathrm{O_I}}$ and $\delta z_{\mathrm{O_{II}}}$ give four possible structures.

The source of this uncertainty can be seen from the following:

$$F^2 = A(\mathrm{Pb})^2+2A(\mathrm{Pb}).[A(\mathrm{Ti})+A(\mathrm{O})] +[A(\mathrm{Ti})+A(\mathrm{O})]^2+[B(\mathrm{Ti})+B(\mathrm{O})]^2;$$

or, expanding:

$$F = A(\mathrm{Pb})\{1+[A(\mathrm{Ti})+A(\mathrm{O})]/A(\mathrm{Pb}) +\tfrac{1}{2}[A(\mathrm{Ti})+A(\mathrm{O})]^2/A(\mathrm{Pb})^2+\tfrac{1}{2}[B(\mathrm{Ti})+B(\mathrm{O})]^2/A(\mathrm{Pb})^2\} .$$

In $PbTiO_3$, either $[A(\mathrm{Ti})+A(\mathrm{O})]$ or $[B(\mathrm{Ti})+B(\mathrm{O})]$ is usually not more than 30% of $A(\mathrm{Pb})$. Therefore, the main contributions to F come from the first and second terms. The third and fourth terms contribute less than 5% each to the total. The change of δz gives a noticeable contribution to F through the second term. However, the change in sign of δz affects only the B term, because the A term contains only $\cos 2\pi l.\delta z$. Thus the contribution to F is through the last term only, and more than a few per cent change in F cannot be expected.

This uncertainty of the sign may be removed by neutron diffraction. As shown in Table 2, the relative

Table 2. *Comparison of atomic scattering factors of* Pb, Ti *and* O *for X-rays and neutrons*

	X-rays (at $\sin\theta/\lambda = 0{\cdot}3\times10^8$)	Neutrons $f_{\mathrm{coh.}}(10^{-12}$ cm.)
Pb	59·5	0·96
Ti	12·8	−0·38
O	3·9	0·58

magnitudes of atomic scattering factors for thermal neutrons (Shull & Wollan, 1951) are quite different from the case of X-rays (*Internationale Tabellen*, 1944), and all of the three are of the same order of magnitude. The contribution of the B term is thus essential to F, and the signs of δz may be determined uniquely. Since a large-enough single-domain crystal for the neutron diffraction study is not available at the present time, a powder diffraction pattern must be used. However, the large lattice distortion may allow resolution even at the low-angle lines. In the following analysis, the X-ray data of the ($h0l$) reflections were used to determine the absolute values of δz, and the neutron powder data were used to decide between the alternative signs.

It should be pointed out that a decision about the signs has never been made in the case of previously published X-ray studies of $BaTiO_3$. Models with $\delta z_{\mathrm{O_I}}$ negative and $\delta z_{\mathrm{O_{II}}}$ either zero or negative have been examined, but no analysis of a model with δz for both O's positive has been presented. While this assumption was apparently correct for $BaTiO_3$, as established by the recent neutron diffraction study at Brookhaven, it will be shown that the same assumption does not hold for $PbTiO_3$.

3. X-ray study

Single crystals of $PbTiO_3$ were grown using PbO as a flux, according to the method described by Rogers (1953). Small but good single crystals were obtained with pseudo-cubic crystal habit. The cell dimensions of these crystals, as determined from a powder pattern picture, agree very well with the previously reported values for ceramic specimens, and the Curie temperature of the crystals was confirmed to be about 490° C. under the polarizing microscope.

Special care was given to selection of crystals for intensity measurements, in view of anticipated large extinction effects. It was not difficult to find single-domain crystals of suitable size which appeared quite perfect under the polarizing microscope. These crystals were avoided, since extinction in them could be expected to be significant. Several multi-domain crystals of the edge length 0·03–0·05 mm. were picked up, and placed on a quartz plate. Using a simple high-temperature optical stage, these were repeatedly heated through the transition at 490° C., until, by chance, one of them became single-domain. By this heat treatment it was hoped that the extinction effects would be minimized. The crystal finally selected by this method had a cross-section of 0·040×0·040 mm., and was 0·060 mm. in length, with the a axis along the longest edge.

The ($h0l$) reflections were collected with a Weissenberg camera, using Mo $K\alpha$ radiation filtered through Zr foil 0·04 mm. thick. The multi-film technique with calibrated intensity scale was used to read off the intensities by visual estimation. A brass sheet of 0·02 mm. thickness was placed between successive films to cut down the intensity. All of the 108 possible ($h0l$) reflections were collected after an eight-day exposure; among them were 17 reflections too weak to be estimated. This gave a range of $\sin\theta/\lambda$ up to 1·4.

Though the crystal used was very small, it was necessary to correct for absorption because of the very high absorbing powder of the Pb atom. The correction was carried out by the graphical method described by Howells (1950). The linear absorption coefficient used was 795 cm.$^{-1}$ for Mo $K\alpha$ radiation.

From the observed intensity I_o, which is already corrected for absorption, the observed structure factor F_o can be calculated:

$$F_o = K\sqrt{\{I_o(Lp)\}} ,$$

where Lp is the Lorentz-polarization factor and K is a scale factor. On the other hand, the structure factor F_c is *calculated* by

$$F_c = \sum_j f_j \exp\left[2\pi i(hx_j+ky_j+lz_j)\right] ,$$

$$f_j = f_{0j} \exp\left(-B_j \sin^2\theta/\lambda^2\right) ,$$

where f_{0j} is the tabulated scattering factor for the atom j at rest (*Internationale Tabellen*, 1944). The disagree-

ment factor R, defined as $R = \Sigma||F_c|-|F_o||\div\Sigma|F_o|$, was used as a criterion for the agreement between F_o and F_c, where the scale for F_o is established by $K = \Sigma|F_c|/\Sigma|F_o|$. First the F_o's were compared with the F_c's with all δz's = 0. This comparison showed that the extinction effect is relatively small and only a few strong reflections with $\sin^2\theta < 0{\cdot}1$ suffered noticeable effect. These reflections were corrected by assuming a secondary extinction effect, and a reasonable result was obtained. Since these reflections have low l values (1 or 2) and are not important to the structure determination in any case, no further efforts were exerted concerning this point.

The R factor for the model with all $\delta z = 0$ is 0·16, indicating relatively large values of δz. Several trial calculations were made by adjusting three coordinate parameters and one temperature parameter, B. In these calculations δz_{Ti} is taken as positive, and both of the signs of δz_{O_I} and $\delta z_{O_{II}}$ are '*assumed*' as negative. It was shown that very good agreement between F_o and F_c can be obtained with

$$\delta z_{Ti} = +0{\cdot}041,\ \delta z_{O_I} = -0{\cdot}110,\ \delta z_{O_{II}} = -0{\cdot}110;$$
$$B = 0{\cdot}57\ \text{Å}^2.$$

Table 3 shows some of the trial F_c calculations with their R values. This shows that oxygen shifts were

Table 3. *Trial structure of tetragonal* $PbTiO_3$

	δz_{Ti}	δz_{O_I}	$\delta z_{O_{II}}$	B (Å²)	R	Q*
$F1$	0	0	0	0·55	0·157	—
$F2$	+0·050	0	0	0·57	0·084	—
$F3$	+0·040	0	0	0·57	0·091	—
$F4(a)$	+0·041	−0·11	−0·11	0·57	0·053	—
$F4(b)$	+0·041	+0·11	+0·11	0·57	0·057	0·011
$F4(c)$	+0·041	+0·11	−0·11	0·57	0·055	0·015
$F4(d)$	+0·041	−0·11	+0·11	0·57	0·054	0·009

* $Q = \Sigma|F4a - F4b$ (or c or $d)|\div\Sigma F4a$.

essential for the improvement of the agreement. Especially, the change is appreciable in the reflections such as (2n,0,4) and (2n,0,6) where three oxygens are in phase for the model with all $\delta z = 0$.

At this stage, the three other possible models resulting from remaining combinations of signs of δz_{O_I} and $\delta z_{O_{II}}$ were examined. The four possible models are shown in Fig. 2. As shown in Table 3, the R factors for all of the four models lie between 0·053 and 0·057, and the difference is certainly too small to be significant. The Q values shown in the last column are also a measure of the very small differences between the structure factors of the four models. Table 4 gives a comparison of the (00l) reflections for these four models, and for the model with all $\delta z = 0$.

It can be concluded that it is not possible to decide between these four models on the basis of the available X-ray intensity. It is quite questionable whether a decision could be reached even with much more precise intensity measurements. An inspection of Fig. 2 could

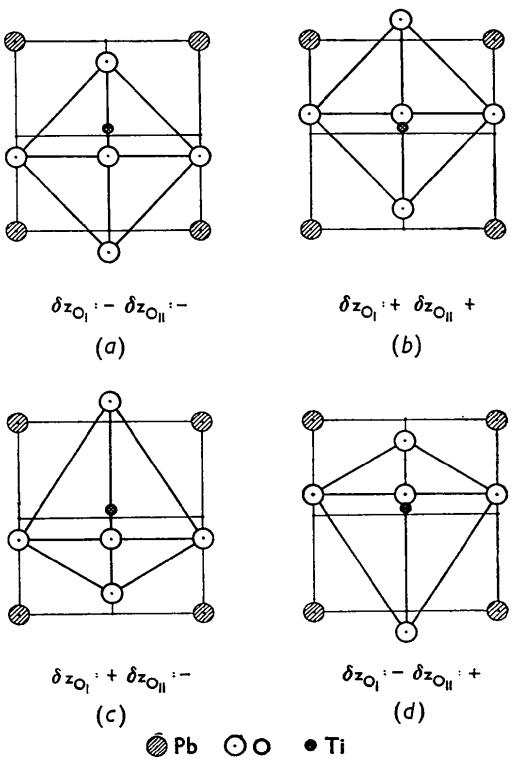

Fig. 2. Four possible structures for tetragonal $PbTiO_3$: $\delta z_{Ti} = +0{\cdot}041$, $\delta z_{O_I} = \pm 0{\cdot}11$, $\delta z_{O_{II}} = \pm 0{\cdot}11$.

Table 4. *Observed and calculated structure factors for* (00l) *X-ray reflections*

F_o is scaled by $\Sigma|F_c|\div\Sigma|F_o|$ using all values for $h0l$. This is practically equal for all five models shown below. The temperature factor B used for the calculation is 0·57 Å² for δz's ≠ 0, and 0·55 Å² for δz's = 0. $\delta z_{Ti} = +0{\cdot}041$, $\delta z_{O_I} = \pm 0{\cdot}11$, $\delta z_{O_{II}} = \pm 0{\cdot}11$

		F_c				
		δz_{Ti} +	+	+	+	0
00l	F_o	δz_{O_I} −	+	+	−	0
		$\delta z_{O_{II}}$ −	+	−	+	0
001	49·3	50·8	51·6	51·8	54·0	48·7
002	75·4	75·5	77·8	75·2	76·0	88·0
003	48·2	43·9	44·7	43·7	46·0	36·7
004	38·1	39·8	40·2	39·7	39·9	54·0
005	33·6	32·7	32·6	32·9	32·4	25·1
006	28·5	26·2	25·1	25·8	25·3	36·0
007	25·0	22·8	23·2	23·3	22·3	16·5
008	17·8	18·1	17·5	17·8	17·6	23·8
009	16·0	14·6	14·6	14·6	14·5	10·2
0,0,10	10·9	10·0	10·2	10·0	10·1	14·4
0,0,11	8·5	9·4	9·4	9·3	9·5	6·2

reveal that the models (*c*) and (*d*) are more improbable because they require drastic changes in O–O distances. Nothing could be concluded from geometrical considerations, however, as to choice between models (*a*) and (*b*), even though model (*a*) has been assumed for $BaTiO_3$.

It may be worth while to mention that the absolute value of δz can be obtained, without any trial method,

if we take advantage of the very fact that the signs cannot be determined. As shown in § 2, this implies a small contribution of B to F; therefore $F_o \cong |A_o|$ with an error less than 5%. Moreover, A is always positive owing to the heavy Pb at the origin. If we carry out a Fourier synthesis using F_o values as A_o, assuming $B_o = 0$, the resulting Fourier map will have Pb at the origin, a half Ti at $+\delta z_{\mathrm{Ti}}$, another half Ti at $-\delta z_{\mathrm{Ti}}$, and the same situation with the three oxygens. What the B_o term will do in the actual F_o synthesis is to cancel out the ghost half Ti and O atoms, and add to the remaining halves, *according* to our assumption of the signs of δz_{Ti}, $\delta z_{\mathrm{O_I}}$ and $\delta z_{\mathrm{O_{II}}}$; for we set

$$A_o = F_o.A_c/F_c, \quad \text{and} \quad B_o = F_o.B_c/F_c .$$

A Fourier synthesis carried out on X-RAC (Pepinsky, 1952) clearly shows split Ti and three O's, in spite of the presence of the heavy Pb. The coordinates are read off as $\delta z_{\mathrm{Ti}} = 0{\cdot}040$, $\delta z_{\mathrm{O_I}} = 0{\cdot}117$, $\delta z_{\mathrm{O_{II}}} = 0{\cdot}116$. Even better resolution was obtained when the Fourier synthesis was carried out after subtracting f_{Pb} from F_o (Fig. 3). The coordinates given are

$$\delta z_{\mathrm{Ti}} = 0{\cdot}036, \ \delta z_{\mathrm{O_I}} = 0{\cdot}110, \ \delta z_{\mathrm{O_{II}}} = 0{\cdot}111 .$$

These values are in excellent agreement with those obtained by the trial method. Similar results may be obtained from a Patterson synthesis, but probably with less accuracy because of overlapping of the vectors.

This direct method has proved, without any assumption, that the absolute magnitude of the shifts of the oxygens in $PbTiO_3$ is almost equivalent. Thus the structure with $\delta z_{\mathrm{O_{II}}} = 0$, analogous to Kaenzig's structure and Evans' first structure of $BaTiO_3$, is not compatible with the observed intensities of $PbTiO_3$. This does not imply that the $BaTiO_3$ structures are incorrect; it merely shows that neither correspond to the tetragonal $PbTiO_3$ structure.

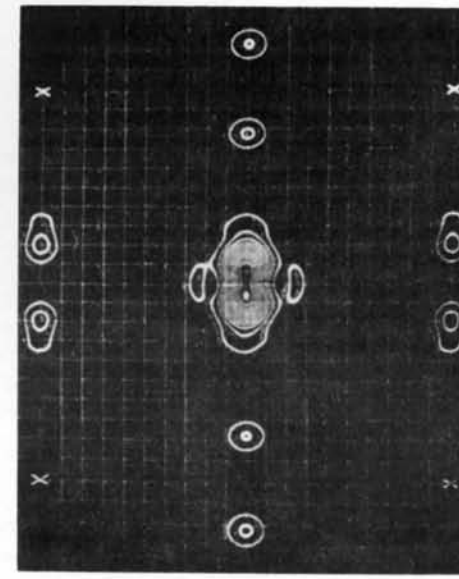

Fig. 3. X-RAC Fourier synthesis for tetragonal $PbTiO_3$, (010) projection, using coefficients $F_o - f_{\mathrm{Pb}}$ as the A term, and assuming $B = 0$. The origin is indicated by crosses.

4. Neutron diffraction study

At this point in the study, neutron diffraction data were collected at the Brookhaven reactor, on material prepared at The Pennsylvania State University. Equimolar parts of $PbCO_3$ and TiO_2 were mixed thoroughly and pressed into pellets. Since it is known that $PbTiO_3$ decomposes and loses PbO at higher temperatures (Rogers, 1953), the pellets were fired at 1000° C. for 2 hr. An X-ray powder pattern of the ceramic was exactly the same as that from powdered single crystals. The ceramic pellets were finely powdered for the neutron diffraction study.

A specimen was placed in a glass cell $\frac{1}{2}$ in. thick, in the transmission arrangement. This was irradiated by a neutron beam 2 in. high and 0·9 in. wide, with a wave length of 1·08 Å. The diffracted intensity was recorded by means of an enriched BF_3 proportional counter, at an interval of $\frac{1}{8}°$ of arc, with ten minutes required for each intensity reading. As shown in Fig. 4, resolution is good enough to permit us to work with nine peaks, involving twelve sets of lattice planes.

For calculation, the following expression was used:

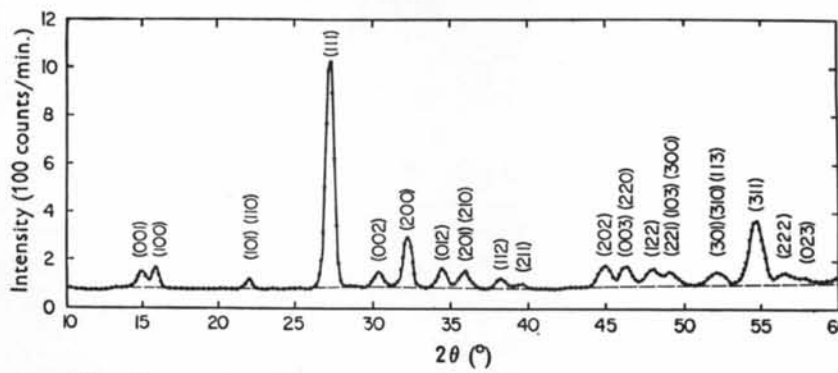

Fig. 4. Neutron powder diffraction pattern of tetragonal $PbTiO_3$. The pattern shown here is taken from the second run referred to at the end of § 5.

$$I_{hkl} = KM_{hkl}F^2_{hkl}\frac{1}{\sin^2 2\theta}\exp[-\mu H \sec\theta] \times \exp[-(2B/\lambda^2)\sin^2\theta],$$

where K is the scaling factor, M the multiplicity, μ the effective linear absorption coefficient, and H the thickness of the specimen. The coherent atomic scattering factors used for the calculation are shown in Table 2. It is clear from this table that neutron data are quite sensitive to the oxygen positions.

The intensities were calculated for four models with $\delta z_{Ti} = +0{\cdot}041$, $\delta z_{O_I} = \pm 0{\cdot}110$ and $\delta z_{O_{II}} = \pm 0{\cdot}110$, which were found to be acceptable from the X-ray study. Since the calculated (100) and (200) reflections must be the same for all models, $[I_c(100)+I_c(200)]$ was scaled to $[I_o(100)+I_o(200)]$. A comparison shows clearly that the only possible model is that with $\delta z_{Ti} = +0{\cdot}41$, $\delta z_{O_I} = +0{\cdot}110$ and $\delta z_{O_{II}} = +0{\cdot}110$ (Table 5). The agreement is excellent for this model and quite unsatisfactory with the other three models.

Table 5. *Observed and calculated powder diffraction intensities of neutrons for* $PbTiO_3$ *for five models*

Values in integrated counts per 0·1 min.
Figures in parentheses $= I^{(obs.)}_{hkl} - I^{(calc.)}_{hkl}$.
$\delta z_{Ti} = +0{\cdot}041$, $\delta z_{O_I} = \pm 0{\cdot}11$, $\delta z_{O_{II}} = \pm 0{\cdot}11$.

		$I^{(calc.)}_{hkl}$				
		δz_{Ti} +	+	+	+	0
		δz_{O_I} +	−	+	−	0
		$\delta z_{O_{II}}$ +	−	−	+	0
hkl	$I^{(obs.)}_{hkl}$					
001	207	217 (−10)	252 (−45)	568 (−361)	455 (−248)	147 (60)
100	224	257 (−33)	257 (−33)	257 (−33)	257 (−33)	257 (−33)
101 } 110	110	111 (−1)	45 (65)	111 (−1)	45 (65)	0 (110)
111	2,625	2,652 (−27)	2,492 (133)	2,245 (380)	2,291 (334)	2,938 (−313)
002	194	202 (−8)	281 (−87)	94 (100)	65 (129)	337 (−143)
200	624	591 (33)	591 (33)	591 (33)	591 (33)	591 (33)
102	290	298 (−8)	379 (−89)	298 (−8)	379 (−89)	111 (179)
201 } 210	216	252 (−36)	277 (−61)	497 (−281)	419 (−203)	206 (10)
112 } 211	182	199 (−17)	91 (91)	457 (−275)	607 (−425)	0 (182)

Calculations are also shown for a model with all $\delta z = 0$. Among nine peaks, the two peaks (101), (110) and (112), (211) are especially sensitive to the oxygen parameters because these reflections have zero intensity when all $\delta z = 0$.

This is a rather unexpected result, since the model with $\delta z_{Ti} > 0$, $\delta z_{O_I} < 0$, $\delta z_{O_{II}} < 0$ has been accepted as a model for $BaTiO_3$. This δz_O's negative model was tried, by adjusting δz_{O_I} and $\delta z_{O_{II}}$ parameters, to obtain better agreement with the observed values; but the attempt was entirely unsuccessful. It is certainly not possible, furthermore, to account for the observed data with the assumption $\delta z_{O_{II}} = 0$.

5. Refinement of the structure

The final refinement of the structure for X-ray data was carried out by Fourier synthesis and the least-squares method. The comparison of the F_o and F_c synthesis carried out with X-RAC shows that: (1) the coordinate parameters are already quite good; (2) the Pb atom is almost isotropic in thermal vibration; (3) the peak height of O_I and O_{II} in the F_o synthesis are somewhat lower than those in the F_c synthesis, by approximately the same amount, indicating that larger temperature factors are required for them. The difference synthesis, $F_o - F_c$, shows essentially the same results.

The least-squares method was applied with respect to the three coordinate parameters and the three isotropic temperature parameters. The temperature parameters for O_I and O_{II} were assumed as equal. The new parameters obtained are shown in Table 6. These results are in good agreement with what was expected from the Fourier method. The structure factors calculated with the new parameters are compared with F_o in Table 7. The f_0's were scaled by $K = \Sigma F_o . F_c / \Sigma F_o^2$.

The R factor for this model is 0·052, and a quadratic mean error ε is 1·95, where ε is defined from $\varepsilon^2 = \Sigma(F_o - F_c)^2/(N-n)$, where N is the number of observations and n the number of parameters. The values given for error in Table 6 are the standard deviations Δx_i calculated from the formula given by Cruickshank (1949):

$$\Delta x_i^2 = (B_{ii}/D)\varepsilon^2,$$

where D is the determinant formed by the quantities $\Sigma(\partial F_c/\partial x_m)(\partial F_c/\partial x_n)$, and B_{ii} is its ith principal minor.

Table 6. *The final refinement of* $PbTiO_3$ *structure by the least-squares method*

	Starting parameters	Final parameters for X-rays	Final parameters for neutrons	'Best parameters'
δz_{Ti}	+0·041	+0·040(±0·002)	+0·038(±0·010)	+0·040
δz_{O_I}	+0·110	+0·113(±0·009)	+0·112(±0·007)	+0·112
$\delta z_{O_{II}}$	+0·110	+0·117(±0·006)	+0·107(±0·005)	+0·112
B (Å²)	0·57	$B_{Pb} = 0{\cdot}57(\pm 0{\cdot}02)$ $B_{Ti} = 0{\cdot}62(\pm 0{\cdot}12)$ $B_{O_I} = 0{\cdot}76(\pm 0{\cdot}24)$ $B_{O_{II}} = 0{\cdot}76(\pm 0{\cdot}24)$	0·57(±0·03)	

Table 7. *X-ray structure factor comparison of (h0l)*

h0l	A_c	B_c	F_c	F_o	*h0l*	A_c	B_c	F_c	F_o	*h0l*	A_c	B_c	F_c	F_o
100	48·5	0	48·5	49·8	503	30·2	2·7	30·3	28·8	007	22·1	−3·3	22·3	25·0
200	84·7	0	84·7	79·6	603	18·7	−3·5	19·0	20·0	107	20·1	4·8	20·7	20·8
300	35·8	0	35·8	39·7	703	19·8	1·6	19·9	19·7	207	20·4	−3·0	20·6	22·1
400	50·3	0	50·3	51·1	803	12·3	−2·1	12·5	9·6	307	17·6	4·1	18·1	19·2
500	23·7	0	23·7	25·3	903	11·9	1·0	11·9	11·7	407	16·8	−2·3	17·0	17·3
600	32·2	0	32·2	35·2	10,0,3	7·0	−1·2	14·4	—	507	13·5	3·3	13·9	13·0
700	15·1	0	15·1	16·2						607	12·2	−1·8	12·3	12·2
800	19·9	0	19·9	21·6	004	39·2	7·8	40·0	38·1	707	9·4	2·2	9·7	—
900	8·9	0	8·9	9·1	104	36·9	−6·6	37·5	37·0	807	8·2	−1·1	8·3	—
10,0,0	11·3	0	11·3	12·1	204	35·3	6·8	35·9	35·4					
					304	30·2	−5·4	30·7	31·2	008	17·7	2·0	17·8	17·8
001	51·0	−9·0	51·8	49·3	404	27·4	5·4	27·9	28·5	108	17·8	−2·6	18·0	17·8
101	77·2	−0·2	77·2	81·0	504	21·6	−4·1	22·0	20·2	208	16·6	1·8	16·7	17·0
201	42·5	−5·5	42·9	43·4	604	19·0	3·7	19·4	18·9	308	15·6	−2·2	15·8	14·6
301	53·1	0·6	53·1	57·3	704	14·6	−2·6	14·8	13·0	408	13·5	1·5	13·6	12·2
401	29·2	−2·8	29·3	29·0	804	11·9	2·2	12·1	11·7	508	12·0	−1·7	12·1	11·5
501	35·0	0·7	35·0	36·7	904	8·9	−1·5	9·0	—	608	9·9	1·1	10·0	9·6
601	18·8	−1·8	18·9	17·8	10,0,4	7·0	1·3	7·1	—	708	8·4	−1·3	8·5	—
701	22·2	0·4	22·2	21·3										
801	11·7	−1·1	11·8	9·9	005	32·3	−5·4	32·7	33·6	009	14·5	−2·0	14·6	16·0
901	13·0	0·2	13·0	12·5	105	35·3	6·4	35·9	36·5	109	11·1	1·8	11·2	12·0
10,0,1	6·8	−0·6	6·8	—	205	29·4	−5·0	29·8	27·2	209	13·5	−1·9	13·6	16·5
					305	29·4	5·4	29·9	28·8	309	9·7	1·6	9·8	—
002	84·1	19·9	76·7	75·4	405	23·0	−4·0	23·3	24·2	409	11·3	−1·6	11·4	10·7
102	47·1	−9·8	48·1	42·6	505	22·0	4·1	22·4	25·6	509	7·7	1·2	7·8	—
202	60·2	13·5	61·7	55·1	605	16·3	−2·7	16·5	19·7	609	8·5	−1·2	8·6	8·0
302	35·4	−6·0	35·9	34·1	705	14·6	2·6	14·8	16·5					
402	41·3	7·6	42·0	40·0	805	10·4	−1·7	10·5	8·5					
502	23·6	−3·8	23·9	22·9	905	9·2	1·5	9·3	—	0,0,10	9·5	2·1	9·7	10·9
602	27·2	5·0	27·6	27·2						1,0,10	11·5	−1·4	11·6	12·2
702	15·1	−2·4	15·3	14·9	006	25·7	2·4	25·8	28·5	2,0,10	8·8	2·0	9·0	—
802	16·8	2·6	17·0	17·3	106	26·3	−4·2	26·6	27·4	3,0,10	10·2	−1·2	10·3	9·1
902	9·0	−1·4	9·1	—	206	23·8	2·1	23·9	23·7	4,0,10	7·5	1·6	7·7	—
10,0,2	9·5	1·6	9·6	9·1	306	22·4	−3·6	22·7	24·8	5,0,10	8·1	−1·0	8·2	7·2
					406	19·4	1·7	19·5	18·9					
003	44·1	−9·0	45·0	48·2	506	17·2	−2·5	17·4	18·1	0,0,11	9·4	−0·9	9·4	8·5
103	56·1	4·2	56·3	52·5	606	13·8	1·1	13·8	15·2	1,0,11	6·5	0·2	6·5	—
203	36·0	−7·3	36·7	38·3	706	11·6	−1·8	11·7	11·4	2,0,11	8·8	−0·8	8·8	6·4
303	43·2	3·5	43·3	42·9	806	8·9	0·7	8·9	—	3,0,11	5·8	0·2	5·8	—
403	27·9	−5·3	28·4	28·5	906	7·3	−1·0	7·4	—					

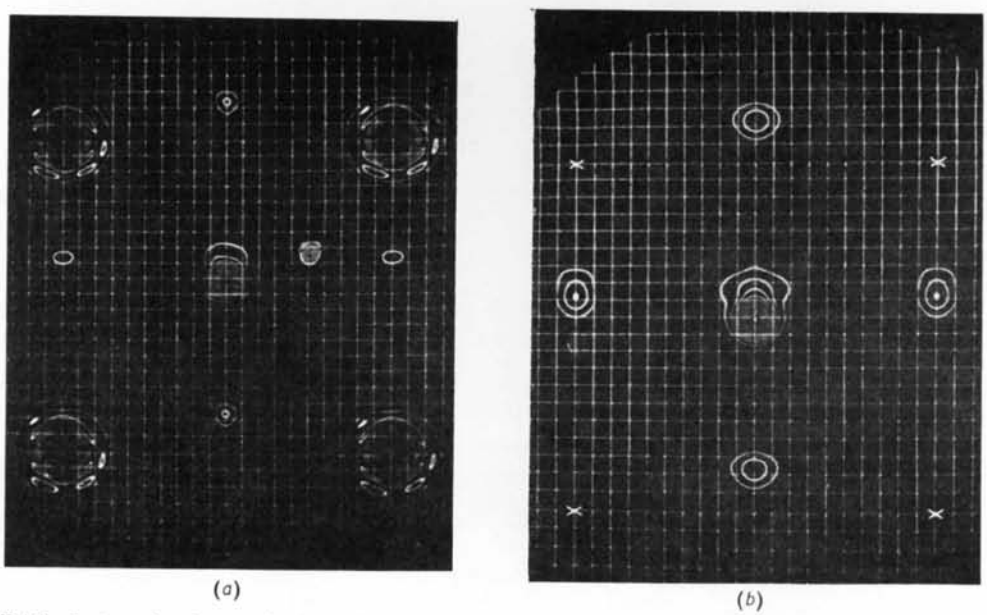

(*a*) (*b*)

Fig. 5. (*a*) X-RAC electron-density projection of tetragonal $PbTiO_3$ on (010). (*b*) X-RAC Fourier synthesis of tetragonal $PbTiO_3$, (010) projection, using coefficients $F_o - f_{Pb}$. The origin is indicated by crosses.

The final F_o synthesis (Fig. 5(*a*)) was carried out with these final parameters. The coordinate parameters read from the map are $\delta z_{Ti} = 0{\cdot}038$, $\delta z_{O_I} = 0{\cdot}114$, and $\delta z_{O_{II}} = 0{\cdot}110$. The series-termination error was corrected by the 'back-shift method', using an F_c synthesis. In this map a strong diffraction effect of the Pb atom, due to the series termination, seems to be appreciable on O_{II}, which lies exactly on the Pb–Pb line. To minimize this effect, f_{Pb} is subtracted from A_o; and the Fourier map thus obtained is shown in Fig. 5(*b*). This $F_o - f_{Pb}$ synthesis shows much better resolution of the oxygen atoms. The parameters read are:

$$\delta z_{Ti} = +0{\cdot}040,\ \delta z_{O_I} = +0{\cdot}114,\ \delta z_{O_{II}} = +0{\cdot}111\ .$$

The least-squares method was also applied to the neutron data. Here, $\Sigma(I_o - I_c)^2$ was minimized, and I_c was scaled by $K = \Sigma I_c I_o / I_c^2$. Only one temperature factor is given because the available intensity data were all at low angles and insensitive to the temperature parameters. The results are shown in Table 6. The standard deviations were estimated by the same method as in the case of the X-ray data, except that the factor $[N/(N-n)]^{\frac{1}{2}}$ was introduced to correct for the small value of N. The final calculated intensities are compared with I_o in Table 8. The quadratic mean error $\varepsilon = 28$.

Table 8. *Comparisons of observed and calculated intensities of neutron diffraction for* $PbTiO_3$

	First run (Counts/0·1 min.)		Second run (Counts/0·5 min.)	
hkl	$I_o - A$	$I_c - A$	$I_o - B$	$I_c - B$
001	207	205	192	206
100	224	254	218	264
101, 110	110	111	99	109
111	2625	2627	2594	2549
002	194	203	214	191
200	624	585	633	563
012	290	305	262	292
201, 210	216	242	247	246
112, 211	182	185	142	129
			68	73
202	—	—	361	353
220, 003	—	—	318	346
122	—	—	304	307
221, 300, 103	—	—	238	249
310, 301, 113	—	—	282	307
311	—	—	1230	1307
222, 023	—	—	347	395

The 'best coordinate parameters' for both the X-ray and neutron data were determined by considering the standard deviation for both cases. More weight is given to the X-ray results for δz_{Ti}, and equal weight is given to both results for oxygen parameters. The best parameters are:

$$\delta z_{Ti} = +0{\cdot}040,\ \delta z_{O_I} = +0{\cdot}112,\ \delta z_{O_{II}} = +0{\cdot}112\ .$$

No further efforts were made concerning the anisotropic temperature factors. It is certain, however, that Pb has no large anisotropic temperature factors. Reliable information on anisotropic temperature factors, especially on Ti and O, may only be obtained from single-crystal analysis by neutron diffraction.

After all these calculations had been completed, a second run of the neutron diffraction pattern was obtained with a better resolution, but with sacrifice of intensity, in order to examine higher-order lines. Although there is some ambiguity as to the background at angles higher than $2\theta = 45°$, the agreement of the calculated values with the 'best parameters' is quite satisfactory (see Table 8).

6. Discussion

One of the most important results of the $PbTiO_3$ analysis is that O_I and O_{II} are shifted, with respect to Pb at the origin, by almost the same amount, 0·47 Å, and in the same direction. Moreover, Ti is shifted by 0·17 Å in the same direction as the three oxygens. This situation appears entirely different from the case of $BaTiO_3$, in which, according to the neutron diffraction study, Ti is shifted by 0·06 Å with respect to Ba, and O_I and O_{II} are shifted by 0·09 Å and 0·06 Å respectively in the opposite direction to the shift of Ti.

It must be emphasized here that it is misleading to express the structure by *the* shifts referring to the *A* atom at the origin. Although the *z* value of the origin is taken quite arbitrarily at the *A* atom, it could actually be at any point along the *z* axis. By fixing the origin at some point, for example at the *A* atom, we are implicity fixing our point of view of the structure. The model with the origin at *A* atom may be convenient for representing the Kaenzig's and Evans' first structures for $BaTiO_3$, because only Ti and O_I are shifted in these. But it is not at all suitable to express the structure of $PbTiO_3$.

The best procedure for $PbTiO_3$, if we need a model

Table 9. *Comparisons of* δz *values for four* $BaTiO_3$ *models and for* $PbTiO_3$

	$z_{O_{II}}$ assumed to be $\frac{1}{2}c$					
	$BaTiO_3$: $a = 3{\cdot}986$ Å, $c = 4{\cdot}026$ Å				$PbTiO_3$: $a = 3{\cdot}904$ Å, $c = 4{\cdot}152$ Å	
	Kaenzig	Evans I	Evans II	Neutron diffraction	This paper	
δz_{O_I} (Å)	−0·13	−0·10	−0·02	−0·04	δz_{O_I} (Å)	0
δz_{Ti} (Å)	+0·06	+0·05	+0·14	+0·12	δz_{Ti} (Å)	+0·30
δz_{Ba} (Å)	0	0	+0·08	+0·06	δz_{Pb} (Å)	+0·47

at all, seems to be to take the origin in such a way that O_{II} are at $\frac{1}{2}c$. This is equivalent, in the case of $PbTiO_3$, to considering that the oxygen octahedron is fixed. Fig. 6 shows the structure of $PbTiO_3$ considered in this way. Notice this figure is inverted, compared with Fig. 2(*b*), in order to show the direction of spontaneous polarization along the $+z$ direction. The structure of $BaTiO_3$ is compared with that of $PbTiO_3$ in Table 9.

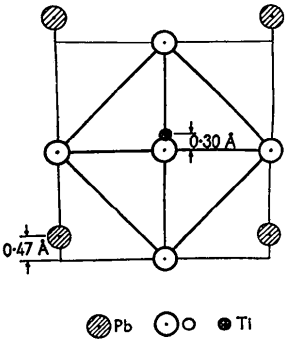

Fig. 6. Crystal structure of tetragonal $PbTiO_3$: oxygen octahedron defining lattice.

From this point of view, the Ti ion in $PbTiO_3$ is shifted by 0·30 Å along the *c* axis with respect to oxygen octahedra, and Pb ions then move in the same direction but by the larger distance of 0·47 Å. The structure of $BaTiO_3$, given by neutron diffraction, indicates a shift of Ti by 0·12 Å and a shift of Ba to the same direction but by a smaller distance of 0·06 Å.

Now let us examine the change in bond length caused by these large shifts of Ti and Pb ions in $PbTiO_3$. For this purpose, Table 10 shows the bond lengths in the cubic structure at 490° C. and those of the tetragonal structure at room temperature. The bond distances are also shown for a ficticious tetragonal structure with all $\delta z = 0$. Passing from the cubic structure above the Curie temperature to the tetragonal structure at room temperature, the oxygen octahedron suffers only the uniform elongation due to the tetragonal distortion, which gives an O_I–O_{II} distance of 2·85 Å and an O_{II}–O_{II} distance of 2·76 Å. The Ti–O_I bond undergoes a drastic change, and Ti–$O_{I(+)}$ bond length

Table 10. *Bond length in tetragonal and cubic* $PbTiO_3$ *structure*

$O_{I(+)}$ means the O_I is close to Ti; $O_{II(+)}$ is close to Pb
All distances in Ångström units

	Tetragonal $\delta z_{Ti} = +0{\cdot}040$ $\delta z_O = +0{\cdot}112$	Tetragonal $\delta z = 0$	Cubic (at 490° C.)
a	3·90	3·90	3·97
c	4·15	4·15	
Ti–$O_{I(+)}$	1·78	2·08	1·98
Ti–$O_{I(-)}$	2·38		
Ti–O_{II}	1·98	1·95	
Pb–O_I	2·80	2·76	2·80
Pb–$O_{II(+)}$	2·53	2·85	
Pb–$O_{II(-)}$	3·20		

becomes 1·78 Å, which is much shorter than the sum of the Goldschmidt radii 1·96 Å (see Fig. 7(*a*)).

Although Pb has the high coordination number of 12, and consequently a large bond distance to surrounding oxygens, the large shift of Pb along the *z* direction brings an appreciable change in the bond length between Pb and O (Fig. 7(*b*)). The Pb–O_{II} length is 2·53 Å, and the sum of the Goldschmidt radii, corrected for 12 coordination, is 2·78 Å. Megaw (1954) emphasized that the homopolar character of the Pb–O bond may play an important role in $PbTiO_3$, and pointed out the homopolar bond system in PbO crystals. In this PbO crystal, Pb–O bonds form a flat tetragonal pyramid with Pb at the apex, and the Pb–O distance is 2·33 Å. The environment of Pb in $PbTiO_3$ may be considered as quite similar to what it is in PbO.

From the observed structure, we can estimate the polarization due to the ion shifts. It is given as $(1/v)\Sigma z_i n_i$, where n_i is the effective charge of the *i*th ion, and *v* is the unit-cell volume. The origin is arbitrarily assigned along *z*; but although individual term changes depend upon the origin, the sum is always constant. Although these n_i's are not known, an assumption of a strictly ionic crystal gives the maximum possible contribution due to ion shift. It is 54 microcoulomb cm.$^{-2}$ for $PbTiO_3$. For $BaTiO_3$, Kaenzig's model and Evans' first and second models give, respectively, 12, 10 and 20 microcoulombs cm.$^{-2}$. It

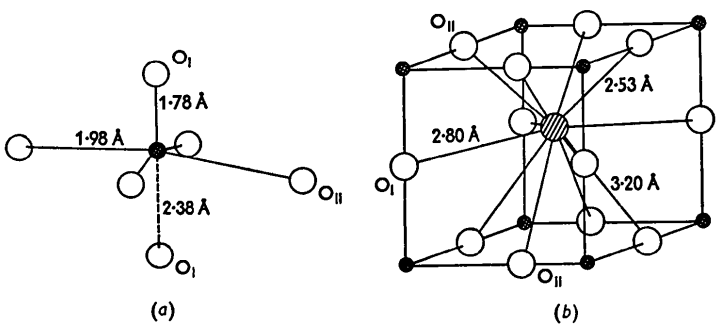

Fig. 7. (*a*) Environment of Ti in $PbTiO_3$. (*b*) Environment of Pb in $PbTiO_3$.

is 17 microcoulombs cm.$^{-2}$ according to the structure given by the neutron diffraction study. The difference between these polarizations and the observed spontaneous polarization are the minimum contribution to be attributed to the electronic polarization. The measured spontaneous polarization of $BaTiO_3$ has been reported (Merz, 1953) as 25 microcoulombs cm.$^{-2}$. Unfortunately no reliable measured value for $PbTiO_3$ is available at present.

One of the important differences between $BaTiO_3$ and $PbTiO_3$ is that the latter shows only one transition at 490° C., while the former shows two additional transitions, at 5° C. and −80° C. These are the transitions to orthorhombic and to rhombohedral phases. Forsbergh (1952) observed that the birefringence of $PbTiO_3$ decreases to one half of its room-temperature value (0·011 for Na light) at liquid-air temperature, and of the order of one third at liquid-helium temperature. It was suspected that this might indicate an associated decrease of lattice distortion with decreasing temperature. Our measurement of the birefringence above room temperature shows this is not the case. As shown in Fig. 8, the birefringence increases gradually, reaches a maximum value of 0·018 at 400° C., and decreases again to 0·012 at the Curie temperature, 490° C. It is not possible to explain this temperature dependence by a combination of the linear and square terms of the spontaneous strain, which increases monotonically with decreasing temperature (Shirane & Hoshino, 1951). This situation is in contrast with the case of $BaTiO_3$, in which the birefringence decreases with increasing temperature in a linear relation to the spontaneous strain. $PbTiO_3$ is optically negative, as is $BaTiO_3$.

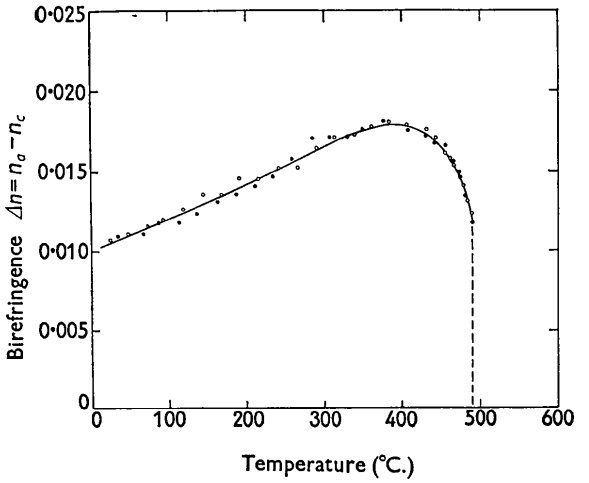

Fig. 8. Temperature dependence of birefringence in tetragonal $PbTiO_3$. Open circles measured by fringes of wedge-type domains; solid circles measured by compensation method, using calibrated quartz wedge (for Na light).

Kaenzig (1955) has suggested that this anomalous optical behavior may be explained as a 'saturation effect of internal field'. This is quite possible in the light of the very large ion shifts observed in $PbTiO_3$. The question that arises immediately is whether this saturation effect occurs only in the optical properties or in the dielectric properties as well. To explore this problem, a theoretical treatment based on the real structure is necessary, together with more experimental information such as the temperature dependence of the spontaneous polarization and of the atomic positions.

The authors are very grateful to Prof. F. Jona and Dr P. F. Eiland for the very illuminating discussions, and to Mr J. McLaughlin for assistance in the calculations. They are equally grateful for the support of this research by the following agencies: the Wright Air Development Center, under Contract No. AF33(616)-2133; the Signal Corps Engineering Laboratories, under Contract No. DA36-039-SC-63233; the Atomic Energy Commission, under Contract No. AT(30-1)-1516; the Office of Naval Research, for X-RAC and S-FAC calculations, under Contract No. N6onr-26916, T. O. 16. The hospitality and assistance of the Brookhaven National Laboratory is deeply appreciated.

References

Cruickshank, D. W. J. (1949). *Acta Cryst.* **2**, 154.
Devonshire, A. F. (1954). *Advances in Physics*, **3**, 85.
Evans, H. T. (1953). *Technical Report No. 58.* Laboratory for Insulation Research, Massachusetts Institute of Technology.
Forsbergh, P. W. Jr. (1952). *Progress Report No. 11*, p. 51. Laboratory for Insulation Research, Massachusetts Institute of Technology.
Frazer, B. C., Danner, H. & Pepinsky, R. (1955). *Phys. Rev.* **100**, 745.
Howells, R. G. (1950). *Acta Cryst.* **3**, 366.
Internationale Tabellen zur Bestimmung von Kristallstrukturen (1944). Ann Arbor: Edwards.
Kaenzig, W. (1951). *Helv. phys. Acta*, **24**, 175.
Kaenzig, W. (1955). Private communication.
Megaw, H. D. (1946). *Proc. Phys. Soc.* **58**, 133.
Megaw, H. D. (1952). *Acta Cryst.* **5**, 739.
Megaw, H. D. (1954). *Acta Cryst.* **7**, 187.
Merz, W. J. (1953). *Phys. Rev.* **91**, 513.
Náray-Szabó, S. (1943). *Naturwissenschaften*, **31**, 466.
Pepinsky, R. (1952). *Computing Methods and the Phase Problem in X-ray Crystal Analysis.* State College: X-ray Crystal Analysis Laboratory of the Pennsylvania State University.
Rogers, H. H. (1953). Technical Report No. 56. Laboratory for Insulation Research, Massachusetts Institute of Technology.
Shirane, G. & Hoshino, S. (1951). *J. Phys. Soc., Japan*, **6**, 265.
Shirane, G. & Suzuki, K. (1951). *J. Phys. Soc., Japan*, **6**, 274.
Shirane, G. & Takeda, A. (1951). *J. Phys. Soc., Japan*, **6**, 329.
Shull, C. G. & Wollan, E. O. (1951). *Phys. Rev.* **81**, 527.